JPET Fast Forward. Published on July 25, 2006 as DOI: 10.1124/jpet.106.109215

JPET #109215

Variability of CYP2J2 expression in human fetal tissues

Andrea Gaedigk, Darren W. Baker, Rheem A. Totah, Roger Gaedigk, Robin E. Pearce, Carrie A. Vyhlidal, Darryl C. Zeldin, and J. Steven Leeder

Division of Clinical Pharmacology & Experimental Therapeutics,

The Children's Mercy Hospital and Clinics, Kansas City, MO (AG, DWB, RG, REP, CAV, JSL)

Department of Medicinal Chemistry, University of Washington, Seattle WA 98195 (RAT)

Division of Intramural Research, National Institute of Environmental Health Sciences, NIH, Research Triangle Park, NC 27709 (DCZ)

Running Title: CYP2J2 mRNA and protein expression in human fetal liver

Corresponding author:

Andrea Gaedigk, PhD
Children's Mercy Hospital
Div Clinical Pharmacology
2401 Gillham Road
Kansas City, MO 64108
Phone: 816-234-3941
Fax: 816-855-1958
Email: agaedigk@cmh.edu

Text pages:
Tables: 3
Figures: 5
References: 26
Words in abstract: 250
Words in introduction: 739
Words in discussion: 1417

Non-standard abbreviations:
ECL, enhanced chemiluminesence; EET, epoxyeicosatrienoic acid; EGA; estimated gestational age, 20-HETE, 20-hydroxyeicosatetraenoic acid; PCR-RFLP, polymerase chain reaction-restriction fragment length polymorphism; SV, splice variant.

Abstract

CYP2J2 metabolizes arachidonic acid to 20-HETE and EETs which play a critical role in the regulation of renal, pulmonary, cardiac and vascular function. However, the contribution of CYP2J2 to EET formation in the liver remains poorly characterized. Similarly, information is sparse regarding the extent and variability of CYP2J2 expression during human development. This investigation was undertaken to characterize the variability of CYP2J2 expression in fetal liver, heart, kidney, lung, intestine and brain and postnatal liver samples. CYP2J2 mRNA expression was measured using quantitative PCR, and immunoreactive CYP2J2 was examined using two anti-CYP2J2 antibodies. CYP2J2 mRNA was ubiquitously expressed in pre- and postnatal samples. Fetal hepatic mRNA expression varied 127-fold (1351 ± 717 transcripts/ng total RNA), but this variation was reduced to 8-fold after exclusion of four samples with extremely low levels of mRNA. Amounts of immunoreactive protein also varied substantially among samples without an apparent relationship with transcript number or genotype. Western blot analysis revealed a different protein pattern between prenatal and postnatal liver samples. DNA resequencing of selected subjects identified a single novel SNP (*CYP2J2*10*), which was found in only one subject and therefore did not explain the large variability in CYP2J2 protein content. In vitro expression suggests that the protein product of *CYP2J2*10* confers reduced enzymatic activity. Aberrant splicing produces three minor transcripts which were present in all samples tested. Due to premature termination codons none encodes functional protein. The mechanisms leading to variable amounts of immunoreactive protein and distinct pre- and postnatal CYP2J2 protein patterns warrant further investigation.

Introduction

Arachidonic acid products 20-hydroxyeicosatetraenoic acid (20-HETE) and 5,6-, 8,9-11,12, and 14,15-epoxyeicosatrienoic acids (EETs) play a critical role in the regulation of renal, pulmonary and cardiovascular function. Recent studies have indicated that conversion of arachidonic acid to these metabolites is primarily catalyzed by cytochrome P450 (CYP) enzymes in the brain, lung, kidney, and peripheral vasculature. While several enzymes from different CYP families, among them members of the CYP1A, 2B, 2C, 2D, 2E, 2J, and 4A subfamilies, have been implicated in EET formation, CYP2J2 has emerged as one of the major extrahepatic enzymes in humans. However, its contribution to EET formation in the liver remains poorly characterized. CYP2J2 has also been reported to be expressed in endothelial cells where EETs, in addition to regulating vascular tone, act as anti-inflammatory mediators. The role of CYP-mediated metabolites of arachidonic acid, including those generated by CYP2J2, has been reviewed and summarized in great detail by Roman (Roman, 2002).

There is also evidence that CYP2J2 plays a role in carcinogenesis. Recent investigations have suggested that upregulation of this enzyme, likely through a c-Jun-responsive module, promotes the neoplastic phenotype of carcinoma cells and may be involved in the pathogenesis of a variety of human cancers (Jiang et al., 2005; Marden and Murray, 2005). However, CYP2J2 can also metabolize a number of xenobiotics including the antihistamine drugs ebastine (Hashizume et al., 2002) and astemizole (Matsumoto et al., 2002) contributing to their presystemic elimination in the small intestine. Taken together, CYP2J2 emerges as a crucial enzyme in a number of physiological functions.

The human CYP2J2 cDNA was first cloned and characterized by Wu et al. 1996 (Wu et al., 1996). In vitro expression demonstrated that it metabolized arachidonic acid predominantly via olefin epoxidation to EETs. Immunoblotting studies revealed that it was primarily expressed in heart and, to a lesser extent, in liver, ileum, jejunum, colon and kidney. Furthermore, interindividual variation in the expression of CYP2J2 mRNA in heart and liver was remarkably low. The expression of CYP2J2 in human tissues was subsequently investigated in more detail demonstrating that the enzyme was abundantly expressed in several tissues (Enayetallah et al., 2004). The *CYP2J2* gene was eventually cloned and sequenced, and was found to consist of nine exons similar to most other members of the human *CYP2* family (King et al., 2002). Currently, the Cytochrome P450 nomenclature committee has defined nine allelic *CYP2J2* variants (http://www.cypalleles.ki.se/cyp2j2.htm). *In vitro* expression studies indicated reduced metabolic activity towards both arachidonic acid and linoleic acid for *CYP2J2*2, *3* and **6,* toward arachidonic acid for *CYP2J2*4,* while the *CYP2J2*5* variant did not appear to have altered activity (King et al., 2002). *CYP2J2*7* involves a G>T substitution in the regulatory region at position -76 (-50 of transcription start) which causes the loss of an Sp1 transcription factor binding site. Consequently, this leads to lower amounts of CYP2J2 protein and reduced levels of circulating CYP2J2 epoxygenase metabolites *in vivo* (King et al., 2002; Spiecker et al., 2004). In addition, two novel variants, *CYP2J2*8* and **9,* have recently been discovered in a Korean population, and *in vitro* expressed *CYP2J2*8* was associated with severely compromised activity towards astemizole O-demethylation and ebastine hydroxylation (Lee et al., 2005). The limited allele frequency data available suggest that the majority of reduced-function alleles are rare and that the

occurrence of some alleles may be restricted to certain populations (e.g. *CYP2J2*3-*6* were only detected in individuals of African descent (King et al., 2002) and *CYP2J2*8* and **9* were only detected in Koreans (Lee et al., 2005)). The sole variant that appears to be present in subjects of all ethnicities is *CYP2J2*7* which has been found at frequencies between 0.026 and 0.18 (King et al., 2002; Lee et al., 2005; Wang et al., 2006).

Most studies on CYP2J2 have been performed with adult subjects or adult-derived tissues. Since CYP2J2 appears to play an important role in EET formation, has a wide tissue distribution and is highly conserved (i.e. low degree of polymorphic expression), one may speculate that it also carries out critical functions during human development. However, to our knowledge, there is limited information about prenatal *CYP2J2* gene expression and function. To gain more insight into CYP2J2 expression during human development, we performed quantitative PCR and immunoblot analyses on a large panel of liver samples genotyped for *CYP2J2* and compared expression levels to that in other tissues. We also detected and characterized alternative splice variants, and resequenced selected samples with high and low CYP2J2 protein levels.

Methods

Source of DNA and RNA

Tissue samples were obtained through NICHD-supported tissue retrieval programs, the University of Maryland Brain and Tissue Bank for Developmental Disorders, (Baltimore, MD), and the Central Laboratory for Human Embryology at the University of Washington (Seattle, WA). RNA from 76 liver specimens (n=58, prenatal; n=18, postnatal) and specimens of fetal heart (n=5), lung (n=10), kidney (n=9), gut (n=4), brain (n=3), testis (n=2) and adrenal (n=2) were used for the study. The use of these tissues was approved by the University of Missouri-Kansas City Pediatric Health Sciences Review Board. 'Brain' refers to cerebrum or cerebellum and was derived from midsections 5, 7, 9, 11 or 13 (all from the University of Maryland). The fetal samples of this study are essentially the same as described previously (Leeder et al., 2005). The post-mortem interval was <6 hours for all samples.

Genomic DNA (n=376) was derived from liver tissue (n=76), or discarded or anticoagulated blood obtained for routine clinical management of hospitalized patients (Caucasians, n=128; African Americans, n=128; American Asians, n=44). Ethnicity was self-reported or retrieved from data sheets accompanying the tissues. The protocol for sample collection and usage was approved by the University of Missouri-Kansas City Pediatric Health Sciences Review Board.

DNA isolation and genotyping for CYP2J2

DNA was isolated using DNeasy Tissue or QIAamp Blood DNA kits (Qiagen, Valencia, CA). Genotyping was performed by PCR-RFLP. Assays were designed *de novo* using

GenBank accession AF272142 as reference sequence. Details including primer sequences and PCR reaction conditions are given in Table 1. PCR amplifications were performed with JumpStart REDTaq DNA polymerase (Sigma, St. Louis, MO) at 1.5 mM $MgCl_2$ with the buffer provided or at optimized $MgCl_2$ concentrations (Table 1). Fragment lengths, restriction enzymes used and restriction patterns for respective assays are shown in Table 2. Restriction enzymes and the 100 bp DNA ladder were purchased from New England Biolabs (Beverly, MA). Digested PCR fragments were separated on 3% agarose gels containing Synergel (Diversified Biotech, Boston, MA).

RNA isolation and quantitative real-time (QRT)-PCR analysis

Total RNA was extracted from frozen tissue (20-35 mg) according to the Qiagen RNeasy protocol (Qiagen, Valencia, CA) with an on-column DNase I treatment. RNA quality was assured by agarose gel electrophoresis and quantity measured spectrophotometrically. QRT-PCR was performed with the QuantiTect SYBR green one-step RT-PCR kit from Qiagen on a DNA Engine Opticon 2 instrument (MJ Research, Boston, MA). Each 12 µl reaction contained 15 ng RNA and was carried out in triplicate. Primers and annealing temperatures are given in Table 1. Serial dilutions of a *CYP2J2* amplicon served as standard to generate a calibration curve ranging from 10^2 to 10^7 molecules. Transcript numbers were calculated from log-linear regression analysis of the calibration curve. Data were normalized to 18S rRNA which was measured with the TaqMan Ribosomal RNA Control Reagent Kit (Applied Biosystems, Foster City, CA).

Immunodetection of CYP2J2 protein

Microsomal fractions were prepared from prenatal and postnatal liver as described previously (Leeder et al., 2005). Microsomal samples were heated to 80°C for 10 minutes. Microsomal proteins (4 μg per lane) were separated using the Novex NuPAGE System (10 well 4-12% gradient gels, XCell SureLock Mini-Cell apparatus, LDS sample buffer, sample reducing agent, antioxidant, MOPS SDS running buffer; Invitrogen, Carlsbad, CA) or the Criterion XT System (18 well 10% Criterion XT gels, Criterion Cell apparatus, XT sample buffer, reducing agent, MOPS running buffer; Bio-Rad, Hercules, CA). Proteins were separated at 150 or 180 volts for 3 hours when using the Novex and Criterion systems, respectively. Proteins were transferred to Hybond-C Extra Nitrocellulose (Amersham Biosciences, Piscataway, NJ) using a Bio-Rad Semi-dry transfer unit with transfer buffer consisting of 48 mM Tris, 39 mM glycine, 20% methanol, 0.0375% SDS at pH 9.2. Membranes were blocked overnight at room temperature on a rocker in 10 mM Tris, 150 mM NaCl, 0.2% Tween 20, pH 8 (TNT) containing 4% skim milk powder (M-TNT). Blocked membranes were incubated for 2 hours with CYP2J2 antibodies designated as anti-CYP2J2rec (Wu et al., 1996) or anti-CYP2J2pep3 (Seubert et al, 2004) diluted 1:50,000-fold in M-TNT and alternately washed in TNT and H_2O (5 min X 3 TNT/H_2O wash cycles). The anti-CYP2J2rec antibody was made against a partially purified preparation of human CYP2J2 protein and has been shown to cross-reacts with CYP2J proteins of multiple species, but not with non-CYP2J isoforms. The anti CYP2J2pep3 antibody was raised against a peptide common to all CYP2J isoforms (see (King et al., 2002) for details). To detect bound antibody, blots were incubated with horseradish peroxidase-conjugated donkey anti-

rabbit antibody (1:50,000) (Amersham Biosciences, Piscataway, NJ) in M-TNT for 30 min, then alternately washed in TNT and H_2O (5 min X 3 TNT/H_2O wash cycles), incubated with ECL Advance chemiluminescense reagents according to the manufacturer's protocol (Amersham Biosciences, Piscataway, NJ), and exposed to Hyperfilm ECL. Films were scanned using a flat-bed scanner. Heterologously expressed CYP2J2 protein (BD Gentest, San Jose, CA) was present on each membrane as a positive control. Each sample was run twice to ensure reproducibility.

cDNA synthesis

Reverse transcription was performed on 2 µg total RNA with an oligo (dT) primer using the Qiagen Omniscript RT kit. Reaction volumes were 20 µl. Subsequent CYP2J2 transcript-specific PCR reactions (full length or partial) were carried out on 0.4 µl cDNA in 8 µl reactions (Table 1).

Amplification, cloning and characterization of CYP2J2 transcripts

Full length CYP2J2 cDNA was amplified in a long-range PCR reaction to allow generation of fragments shorter and longer than the expected wild-type 1.57 kb transcript, should such transcripts exist. Subsequently, cDNA from two samples (one prenatal testis, one postnatal liver) containing potential variant transcripts was cloned with the pCR-XL-TOPO cloning kit designed for efficient cloning of larger amplicons (Invitrogen, Carlsbad, CA) and screened for insert length. Clones with inserts deviating in size from that of correctly spliced mRNA were further analyzed by DNA sequencing

with DYEnamic ET dye terminator chemistry and a MegaBACE 500 capillary sequencer (Amersham Biosciences, Piscataway, NJ).

To detect differentially spliced variants in panels of cDNAs from various tissues, we designed primers amplifying the affected regions. The reaction for splice variants SV2 and SV3 generated three fragments identifying correctly spliced, exon 7A deleted and exon 7B retained transcripts, respectively, while the reaction for SV4 yielded two PCR products corresponding to correctly spliced and exon 2 deleted transcripts, respectively. Primers and other reaction details are given in Table 1.

CYP2J2 gene resequencing

Four long-range PCR products ranging from 5.3 to 8.7 kb in length and covering all exons as well as flanking intronic and the 3'and 5'-untranslated regions were generated (Table 1). The fragments were treated with Exo/SAP-IT (USB, Cleveland, OH) and subsequently sequenced with DYEnamic ET dye terminator chemistry and a MegaBACE 500 capillary sequencer using appropriately spaced *CYP2J2* primers to cover all exons, at least 100 bp of flanking intronic, 550 bp upstream and 375 bp of downstream sequence, respectively.

Automated splice site analysis

The strengths of splice sites and splice enhancer binding sites were determined by automated analysis available at https://splice.cmh.edu using models based on the April 2003 release of the Human Genome Sequence (Build 33). According to the models,

donor and acceptor splice sites are defined by an information content (Ri value) >0 bit (Rogan et al., 1998; Nalla and Rogan, 2005).

*In vitro expression and characterization of CYP2J2*10*

The CYP2J2 cDNA was expressed in the bacterial expression vector PCW+ (source pCWhum3A4HT, (Guryev et al., 2001)) after truncation of the N-terminus and addition of a hexahistidine tag to the C-terminus to facilitate purification (wild-type construct, CYP2J2.1). The $P_{115}L$ amino acid change was introduced into the wild-type construct using the primers: 5'-CCGCCCCGTGACCCTTATGCGAGAACATA 3' and 3-TATGTTCTCGCATAAGGGTCACGGGGCGG-5' (the changed nucleotide is underlined) with a QuickChange II XL site directed mutagenesis kit (Strategene, La Jolla, CA) according to the manufacturer's instructions. The integrity of the variant construct was confirmed by DNA sequencing. Protein expression was performed as previously described (Cheesman et al., 2003) and also in the presence of chaperone proteins (GroES-GroEL) (Mitsuda and Iwasaki, 2006). Expressed CYP2J2 protein was affinity purified using a Ni-NTA agarose column from Qiagen (Valencia, CA) and eluted fractions were dialyzed against 100mM Potassium phosphate buffer, pH 7.4, containing 20% glycerol prior to storage in 15-20 μM aliquots at −80 °C. Heme content in these preparations was determined using the pyridine hemochromagen assay of sodium dithionite reduced heme (Smith, 1975). Details of the bacterial expression and purification systems will be described elsewhere (Jones et al., in preparation).

Statistical Analyses

Analyses were performed with the SPSS version 12.0 software package for Windows (SPSS Inc., Chicago, IL). A normal distribution was established by Q-Q-Plot for the number of transcripts/ng total RNA. Univariate analyses of variance were performed using log-transformed values for number of transcripts/ng total RNA. To assess whether expression levels differed among tissues, a mixed model analysis with a Bonferroni adjustment for multiple comparisons was performed. Linear regression analysis was performed with Microsoft Excel 2002. A p-value <0.05 was considered statistically significant.

Results

CYP2J2 genotyping

All subjects for which tissue was available (n=76) were genotyped for *CYP2J2*2* through **7*. No *CYP2J2*2, *3, *4, *5,* or **6* alleles were found in any of the samples. *CYP2J2*7*, however, was observed at a frequency of 0.099 in this ethnically mixed population (Caucasian, n=35; African American, n=25; other or unknown, n= 16).

Variability in CYP2J2 gene transcription

Expression of CYP2J2 mRNA is reported as transcripts per nanogram total RNA corrected for the expression of 18S rRNA as recommended by Koch et al. (Koch et al., 2002) and as applied previously to fetal liver CYP3A expression (Leeder et al., 2005). As shown in Fig. 1A, expression varied 127-fold in the panel of human fetal liver samples (n=58). Mean ± SD (range) expression was 1351 ± 717 transcripts/ng total RNA (23 to 2957 transcripts/ng total RNA). A subset of four samples had markedly reduced levels of CYP2J2 mRNA, of which three samples (CMM311, CMM32, CMM361) subsequently were found to be devoid of immunoreactive protein while the fourth sample, CMM1153, did reveal protein. These four samples were significantly different when compared to the remaining 54 samples (p=0.001). These samples have been previously reported to contain extremely low levels of CYP3A7 mRNA, immunoreactive protein and catalytic activity (Leeder et al., 2005). In the subset of 54 samples mRNA expression was normally distributed, and the level of expression was not affected by age, either estimated gestational age (r^2 =0.047) or postnatal age (r^2 =0.0003). When excluded from the

analysis, variability in *CYP2J2* mRNA expression decreased from 127-fold to 8-fold (n=54). Furthermore, there was no statistically significant difference between the pre- and postnatal groups regardless whether the four samples described above were included (p=0.86) or excluded (p=0.17) from the analysis. In the 18 postnatal samples (ranging from 4 days to 18 years of age), mRNA expression varied only 19-fold (mean ± SD, 1482 ± 1229 transcripts/ng total RNA, range: 253 to 4728 transcripts/ng total RNA). The lowest transcript number was observed in a sample from a 16 day-old infant that was homozygous for the *CYP2J2*7* allele. We also noted that this sample exhibited some RNA degradation and it was not conclusive whether the low transcription level was due to the genotype or RNA quality. Exclusion of this sample decreased the variability to 15-fold; mean ± SD (range) expression was 1554 ± 1227 transcripts/ng total RNA (326 to 4728 transcripts/ng total RNA). Genotype, i.e. the presence of the *CYP2J2*7* allele did not impact the number of transcripts/ng total RNA. As shown in Figure 2, there was no statistically significant difference between the two genotype groups in either the fetal (p=0.37) or postnatal group (p=0.67).

Smaller panels of extra-hepatic tissues were also investigated and demonstrated that CYP2J2 was ubiquitously expressed in the fetus (Fig 1B). QRT-PCR revealed the highest expression levels in prenatal heart (n=5, mean ± SD 1735 ± 1777 transcripts/ng total RNA) and intestine (n=4, mean ± SD 356 ± 213 transcripts/ng total RNA) followed by lung (n=10, mean ± SD 56 ± 32 transcripts/ng total RNA) and kidney (n=9, mean ± SD 75 ± 135 transcripts/ng total RNA). Lowest levels were observed in brain (n=3; 2, 8 and 18 transcripts/ng total RNA). Univariate analysis of variance revealed that mRNA expression was comparable between liver and heart (p=1.0) or intestine (p=0.15), but was

significantly greater than that observed in lung ((p=0.001) and kidney (p=0.001). No statistically significant difference was observed between lung and kidney. The outcome did not change when all samples derived from the four subjects with low liver mRNA (circled in Figure 1A) were excluded from the analysis.

Variability in CYP2J2 immunoreactive protein

Immunoreactive protein content was assessed in 51 prenatal and 18 postnatal liver microsomal samples. Representative immunoblots illustrating the range of immunoreactive CYP2J2 content in samples ranging from 11.1 weeks of gestation to 17 years of life is shown in Fig 3A. Of note, the polyclonal anti-CYP2J2rec antibody recognized two predominant immunoreactive proteins in the postnatal samples and in one prenatal sample (CMM1153; 32 weeks EGA). Upon close inspection, some samples revealed an additional minor band. This band pattern has been observed previously in adult liver microsomes, but not in heart microsomes (Wu et al., 1996). In contrast, the lower molecular mass protein was not observed in all other fetal liver samples. The CYP2J2pep3 anti-peptide antibody consistently recognized two proteins in the fetal samples while the postnatal pattern consisted of multiple bands of variable intensities (Fig 2B). Of note, sample CMM1153 again exhibited a pattern resembling that observed in postnatal microsomes. These data suggested the presence of novel CYP2J2 isoform(s) or alternatively, the presence of an unrelated protein with an epitope(s) recognized by both CYP2J2 antibodies used.

Despite comparable CYP2J2 mRNA transcript levels in the prenatal and postnatal liver samples, the amount of immunodetectable protein was considerably lower in the fetus. As a consequence, a longer exposure time was needed to visualize immunoreactive CYP2J2 protein in prenatal samples compared to the postnatal samples (30 sec exposure vs. 10 sec, respectively). The extent of this phenomenon can be appreciated in Fig 3A and 3B by comparing the intensity of the signal for the 0.1 pmol standard of recombinant CYP2J2 protein included in each panel.

Considerable variability in protein content was also observed among the panel of prenatal samples. This finding is summarized in Figure 4. The amount of immunoreactive protein ranged from 'low' (including non-detectable) to 'intermediate' and 'high' (by visual inspection, categories used for descriptive purposes only). The 'low' protein bands approximated 0.006 pmol of CYP2J2 protein per µg microsomal protein, while the strongest bands in the 'high' protein category were between 0.012 and 0.02 pmol of CYP2J2 protein per µg microsomal protein. No relationship between transcript number and the amount of immunoreactive protein was apparent across the panel of 51 samples (not shown).

CYP2J2 splice variants and automated splice site analysis

Because mRNA expression appeared to be comparable in prenatal and postnatal liver and immunoreactive protein expression patterns were variable, we explored the possibility that developmentally regulated alternative splicing may lead to reduced expression of the canonical transcript and thus, translation into CYP2J2 protein in prenatal liver. Therefore, full-length cDNA was amplified from a panel of tissue samples. The canonical

transcript, as well as amplification products that were smaller and larger than the correctly spliced transcript, were detected in all samples implying the presence of alternative splice products (Fig 5A). Cloning and sequencing the cDNA from two tissue samples (prenatal testis and postnatal liver) with appreciable levels of the variant transcripts revealed three novel splice variants (Fig 5B). Two variants, SV2 and SV4, had deletions of exon 2 and exon 7, respectively, while SV3 retained a cryptic exon. To discriminate the canonical exon 7 from the cryptic exon 7, they have been designated as exons 7A and 7B, respectively. Both exon deletions and the retention cause frame shifts and introduce premature stop codons.

Splice variants SV2 and SV3 were minor transcripts and difficult to visualize by gel electrophoresis, but appeared to be present in all tissues tested (not shown). In contrast, PCR amplification specific for the exon 2 deletion variant (SV4) did not reveal any visible product in a panel of tissues including the two subjects from which it was originally cloned (CMM684 and CMM1409), suggesting that it constitutes only a rare variant (not shown).

The strengths of the splice donor and acceptor sites were calculated with the information theory-based splice site analysis tool that we have successfully applied to the analysis of other CYP splice sites (Rogan et al., 2003; Gaedigk et al., 2005) (Table 3). Each canonical donor and acceptor splice site contained at least 3.7 bits of information. The exon 2 and exon 7A deletions could not be explained by the presence of weak splice acceptor or donor sites. However, the observed splice junctions of the cryptic exon 7B corresponded to strong 9.0 bit and 5.2 bit acceptor and donor sites, respectively, as predicted by splice site analysis.

The variability in fetal liver CYP2J2 protein expression patterns was unlikely due to SV2, SV3 and SV4, since these splice variants were minor and rather ubiquitously present across tissues. Therefore, we searched for additional splice variants, which may have escaped our initial cloning/screening experiments. However, amplification of cDNA covering exons 2 through 9 and exons 2 through 7A did not reveal any additional splice products in samples classified as 'high' (n=3), 'intermediate' (n=2) and 'low' (n=3) protein expression. The samples used for this analysis corresponded to those shown in Figure 4.

*Discovery and characterization of the novel CYP2J2*10 allele*

A nonsynonymous C>T SNP was discovered at AF272142 g.16810 (cDNA position 344) when selected DNA samples with 'low' levels of immunoreactive protein were resequenced. This SNP was detected in a single subject of unknown ethnicity (CMM1059) and was confirmed by sequencing multiple PCR-generated templates as well as by PCR-RFLP genotyping. Subsequent genotyping of the tissue DNA panel (n=76 including the carrier) and an additional set of DNAs including 128 Caucasians, 128 African Americans and 44 American Asians (total of 600 alleles) did not reveal any other carrier, making this allele a rare event. The novel allele was designated as *CYP2J2*10* by the P450 Nomenclature Committee at http://www.cypalleles.ki.se/cyp2j2.htm.

To assess the functional consequence of the $P_{115}L$ amino acid substitution, CYP2J2.10 protein was expressed in the presence and absence of chaperone proteins GroEL/GroES using a bacterial expression system. Based on protein content, expression with the chaperones yielded 432 and 345 nmol/L CYP2J2 wild-type and CYP2J2.10 protein,

respectively. SDS-PAGE analysis with the CYP2J2pep3 antibody showed a protein band at 57 kDa that was identical in size to that derived from the wild-type cDNA and both expressed proteins. However, CYP2J2.10 appeared to be devoid of heme as judged by the lack of a P450 CO-difference spectrum at 450nm and the presence of a large absorbance peak at 280nm (not shown). Moreover, the ratio of free to protein-bound heme revealed only trace amounts of heme in the CYP2J2.10 preparation, while heme was readily incorporated into wild-type protein (ratios of 0.87 and 0.02 for wild-type and CYP2J2.10, respectively). These results strongly indicate that $P_{115}L$ affects proper heme binding or protein folding. Therefore, CYP2J2.10 protein activity is likely severely compromised. Preliminary results using terfenadine as a probe substrate for CYP2J2 activity corroborate our findings and further support our conclusion that CYP2J2.10 protein activity is likely severely compromised (Jones et al., in preparation). An alignment of CYP2 family members including human, rat and rabbit sequences showed that P_{115} is located within the substrate recognition site (SRS)-1 that proceeds the formation of the B'-helix, but it does not appear to be highly conserved. At this point in time, however, it remains speculative whether P_{115} is important for protein folding and/or heme binding.

Discussion

The findings of this study demonstrate that CYP2J2 mRNA is expressed in human fetal liver as early as 11 weeks EGA, expression levels are comparable to those observed in fetal heart, interindividual variability is relatively low and there is no apparent change in the level of expression after birth. Furthermore, transcript was also detected in every other extrahepatic tissue tested, albeit at lower levels. In contrast to the apparently tight regulation of gene transcription in fetal liver (Fig 1A), there were marked differences in the amount of immunoreactive protein present in this tissue (Fig 3 and 4). Taken together, this suggests that processes other than transcription regulate variability in CYP2J2 protein content. Unfortunately, to date there is no validated CYP2J2 probe substrate available that would allow specific determination of CYP2J2 catalytic activity. Certain antihistamine drugs, including ebastine and astemizole, are known to be metabolized by CYP2J2, but other P450s such as CYP3A4, CYP4F and CYP2D6 have been reported to contribute to the metabolism of these substrates (Hashizume et al., 2002; Matsumoto et al., 2002). While CYP3A4 and CYP2D6 are not expressed at appreciable amounts in fetal liver, their contribution to fetal ebastine and astemizole metabolism may be negligible. However, CYP3A5 and CYP3A7, which are present in fetal liver (Leeder et al., 2005) and CYP4F family members, which likely are also expressed prenatally, given their importance in fatty acid epoxide inactivation (Le Quere et al., 2004) may contribute to the overall activity measured towards ebastine and astemizole and therefore render these probes nonspecific. Efforts to overcome these challenges are currently underway.

We also detected different pre- and postnatal protein expression patterns. In the postnatal liver samples, the anti-CYP2J2 antibody recognized two or three distinct bands, which is

similar to the observations of Wu et al. in adult liver using the same antibody (Wu et al., 1996). Interestingly, a predominant immunoreactive protein was detected in the fetal liver tissue samples, similar to the results reported by Wu et al. in adult heart. These authors speculated that adult liver contains additional CYP2J2 isoforms and/or other proteins that share immunochemical determinants with CYP2J2, but their nature remains elusive. Regardless, it appears that protein expression in adult heart resembles that in fetal liver and that there is a distinct pattern in postnatal liver. Differential protein patterns between pre-and postnatal liver were also observed with a second antibody, anti-CYP2J2pep3, providing further evidence that these developmental differences are real. On the other hand, Gu et al. found only a single immunoreactive band in fetal olfactory mucosa (n=8) and liver (n=6) as well as in their single adult control sample using an anti-rat Cyp2J4 antibody (Gu et al., 2000). We can only speculate at this point in time whether the anti-rat Cyp2J4 antibody is indeed more specific compared to the antibodies used in this study and others (Wu et al., 1996; Yu et al., 2000; King et al., 2002; Jiang et al., 2005) or fails to detect certain CYP2J2 postnatal liver-specific isoforms. Clearly, further studies are required to determine if the various proteins recognized by the CYP2J2 antibodies are indeed isoforms and if so, to characterize their functional properties in a developmental context.

The four samples with low CYP2J2 transcript numbers (Fig 1A) were derived from fetuses with severe congenital anomalies. These samples also presented with low CYP3A7 mRNA expression, protein content and activity. As described and discussed in detail by Leeder et al., 2005, these observations could not be explained by poor sample quality. Noteworthy is sample CMM1153, which demonstrated a pattern of

immunoreactivity unlike the other three samples (Fig 1A and 3), but very similar to that observed in postnatal samples. This unique presentation of a 'fetal' sample may be explained by compromised viability due to porencephaly or other unknown factors.

In order to explain the variability in protein content, the liver panel was genotyped for *CYP2J2*2* through **7* by PCR-RFLP. The only variant found was the more common *CYP2J2*7* allele, which could not explain the variable amounts of protein. Therefore, we performed gene resequencing on eight subjects with high, intermediate and low protein levels, but no sequence variations explaining the variable amounts of protein were revealed. Only a single novel SNP at position AF272142 g.16810 was discovered in one subject of unknown ethnicity. Subsequent genotyping of the liver panel and additional Caucasian, African American and Asian samples totaling 600 chromosomes, did not reveal any additional carriers of this novel allele termed *CYP2J2*10*. The failure to detect any additional novel SNPs within the coding and 100bp of intronic sequences is consistent with previous studies which discovered few sequence variations at rather low frequencies (King et al., 2002; Spiecker et al., 2004; Lee et al., 2005). However, the presence of a SNP(s) located deep within an intron may explain low levels of protein. Such a scenario is the main cause of CYP3A5 poor metabolism, where a SNP in intron 3 creates a cryptic splice site that leads to a premature stop codon and nonfunctional truncated protein (Kuehl et al., 2001). Since resequencing focused on exons, flanking intron portions and 500 bp of promoter sequence, SNPs outside these regions eluded discovery in this investigation.

Gene reporter studies have demonstrated that the loss of an SP1 binding site on the *CYP2J2*7* allele causes a reduction in transcription level (Spiecker et al., 2004), but the

transcript number/ng total RNA was not significantly different between our homozygous and heterozygous groups, respectively (Fig. 2). At this point we can only speculate whether the functional allele compensates for the reduced expression of *CYP2J2*7* in liver tissue, whether there are additional splice variants that are initiated from a different promoter or whether other factors are at play. Albeit significantly lower concentrations of EET metabolites in plasma have been attributed to the presence of the *CYP2J2*7* allele (Spiecker et al., 2004), this in vivo phenotype reflects EET metabolism of all tissues where CYP2J2 is expressed. Clearly, additional studies on hepatic CYP2J2 activity are warranted.

To assess whether C>T ($P_{115}L$) in *CYP2J2*10* conveys any functional consequences, CYP2J2.10 protein was expressed *in vitro* in a bacterial system (Jones et al., in preparation). Since the majority of apoprotein was devoid of heme, one may speculate that $P_{115}L$ intervenes with heme incorporation *in vivo* and thereby compromises the amount of functional protein. *CYP2J2*10* was found in a composite heterozygote with *CYP2J2*7*, which could explain the low level of immunoreactive protein in this particular sample. Yet, given the rarity of this allelic variant, it did not explain the observed variability and likely does not play a significant role in overall interindividual variation in CYP2J2 levels.

Next, in an effort to detect any aberrant mRNA splice variants, cDNA was amplified from the same subjects (representing high, intermediate and low protein) in whom the *CYP2J2* gene was resequenced. Each revealed a major product corresponding to the correctly spliced mRNA and two minor products. Subsequent analysis on full-length cDNA on a set of tissues from one pre- and one postnatal subject did not reveal any

additional tissue-specific splice products. These findings are also in agreement with the automated splice site analysis shown in Table 3 that calculated relative high bit values for almost all canonical splice sites. None of the three alternate splice variants that were ultimately identified (Fig 5B) encode functional protein due to frame shifts introduced by deletion and retention events. Again, this set of experiments failed to find any explanation for the variability in protein expression. There is no evidence in the literature suggesting that CYP2J2 transcripts include alternative exons at the 5'-end (i.e. other canonical exons 1), but it is conceivable that alternate first exon(s) exist. Such exons were, however, not captured by using primers directed to the known exon 1 sequence. Further characterization of splice events affecting the 5'-ends may ultimately discover additional splice variants that could account for the variable amounts of protein detected. Possibly, such variants may also encode the immunoreactive proteins identified in postnatal and adult liver, but not fetal liver and adult heart.

In summary, we provide an initial characterization of CYP2J2 mRNA and protein expression during human development. While mRNA expression appears to be tightly regulated, immunoreactive protein varies considerably. Furthermore, resequencing of the gene and characterization of splice variants did not provide any explanation for the variability seen on the protein level. Future investigations will be directed towards the development of specific probe substrates to permit assessment of CYP2J2 activity in liver microsomal preparations and more detailed characterizations of mRNA splicing in the 5' and 3'-ends of CYP2J2 transcripts.

Acknowledgement:

We thank Stephen D. Simon, PhD for statistical support.

References

Cheesman MJ, Baer BR, Zheng Y, Gillam E and Rettie AE (2003) Rabbit CYP4B1 engineered for high-level expression in Escherichia coli: ligand stabilization and processing of the N-terminus and heme prosthetic group. *Arch. Biochem. Biophys.* **416**:17-24.

Enayetallah AE, French RA, Thibodeau MS and Grant DF (2004) Distribution of soluble epoxide hydrolase and of cytochrome P450 2C8, 2C9 and 2J2 in human tissues. *J. Histochem. Cytochem.* **52**:447-454.

Gaedigk A, Gaedigk R and Leeder JS (2005) CYP2D7 splice variants in human liver and brain: Does CYP2D7 encode functional protein? *Biochem. Biophys. Res. Comm.* **336**:1241-1250.

Gu J, Su T, Chen Y, Zhang Q-Y and Ding X (2000) Expression of biotransformation enzymes in human fetal olfactory mucosa: potential roles in developmental toxicity. *Toxicol. Appl. Pharmacol.* **165**:158-162.

Guryev O, Gilep A, Usanov S and Estabrook R (2001) Interaction of Apo-cytochrome b5 with Cytochromes P4503A4 and P45017A: Relevance of Heme Transfer Reactions. *Biochemistry* **40**:5018-5031.

Hashizume T, Imaoka S, Mise M, Terauchi Y, Fuji T, Miyazaki H, Kamataki T and Funae Y (2002) Involvement of CYP2J2 and CYP4F12 in the metabolism of ebastine in human intestinal microsomes. *J. Pharmacol. Exp. Ther.* **300**:298-304.

Jiang J, Chen C-L, Card JW, Yang S, Chen J-X, Fu X-N, Ning Y-G, Xiao X, Zeldin DC and Wang DW (2005) Cytochrome P450 2J2 promotes the neoplastic phenotype

of carcinoma cells and is up-regulated in human tumors. *Cancer Res.* **65**:4707-4715.

King LM, Ma X, Srettabunjong S, Graves J, NBradburry JA, Li L, M. S, Liao JK, Mohrenweiser H and Zeldin DC (2002) Cloning of *CYP2J2* gene and identification of functional polymorphisms. *Mol. Pharmacol.* **61**:840-852.

Koch I, Weil R, Wolbold R, Brockmöller J, Hustert E, Burk O, Nuessler AC, Neuhaus P, Eichelbaum M, Zanger UM and Wojnowski L (2002) Interindividual variabilty and tissue-specificity in the expression of cytochrome P450 3A mRNA. *Drug Metab. Dispos.* **30**:1108-1114.

Kuehl P, Zhang J, Lin Y, Lamba J, Assem M, Schuetz J, Watkins PB, Daly A, Wrighton SA, Hall SD, Maurel P, Relling M, Brimer C, Yasuda K, Venkataramanan R, Strom S, Thummel K, Boguski MS and Schuetz E (2001) Sequence diversity in *CYP3A* promoters and characterization of the genetic basis of polymorphic CYP3A5 expression. *Nature Genetics* **27**:383-391.

Le Quere V, Plee-Gauter E, Potin P, Madec S and Salaun JP (2004) Human CYP4F3s are the main catalysts in the oxidation of fatty acid epoxides. *J. Lipid Res.* **45**:1446-1458.

Lee SS, Jeong HE, Liu KH, Ryu JY, Moon T, Yoon CN, Oh SJ, Yun CH and Shin JG (2005) Identification and functional characterization of novel CYP2J2 variants: G312R varaint causes loss of enzyme catalytic activity. *Pharmacogenet. Genomics* **15**:105-113.

Leeder JS, Gaedigk R, Marcucci KA, Gaedigk A, Vyhlidal CA, Schindel BP and Pearce RE (2005) Variability of CYP3A7 expression in human fetal liver. *J. Pharmacol. Exp. Ther.* **314**:626-635.

Marden NY and Murray M (2005) Characterization of a c-Jun-responsive module in the 5'-flank of the human CYP2J2 gene that regulates transactivation. *Biochem. J.* **391**:631-640.

Matsumoto S, Hirama T, Matsubara T, Nagata K and Yamazoe Y (2002) Involvement of CYP2J2 on the intestinal first-pass metabolism of antihistamine drug, astemizole. *Drug Metab. Dispos.* **30**:1240-1245.

Mitsuda M and Iwasaki M (2006) Improvement in the expression of CYP2B6 by co-expression with molecular chaperones GroES/EL in Escherichia coli. *Protein Expr. Purif.* **46**: 401-405.

Nalla VK and Rogan PK (2005) Automated splicing mutation analysis by information theory. *Human Mutation* **25**:334-342.

Rogan PK, Faux BM and Schneider TD (1998) Information analysis of human splice site mutations. *Human Mutation* **12**:153-171.

Rogan PK, Svojanovsky S and Leeder JS (2003) Information theory-based analysis of CYP2C19, CYP2D6 and CYP3A5 splicing mutations. *Pharmacogenetics* **13**:207-218.

Roman RJ (2002) P-450 metabolites of arachidonic acid in the control of cardiovascular function. *Physiol. Rev.* **82**:131-185.

Smith K (1975) *Porphyrins and Metalloporphyrins.* Elsevier Science, Amsterdam.

Seubert J, Yang B, Bradbury A, Graves J, Miller L, Gabel S, Gooch R, Foley J, Newman J, Mao L, Rockman HA, Hammock BD, Murphy E and Zeldin DC (2004) Enhanced postischemic functional recovery in CYP2J2 transgenic hearts involves mitochondrial ATP-sensitive K^+ channels and p42/p44 MAPK pathway. *Circ. Res.* **95**:506-514.

Spiecker M, Darius H, Hankeln T, Soufi M, Sattler AM, Schaefer JR, Node K, Borgel J, Mugge A, Lindpaintner K, Huesing A, Maisch B, Zeldin DC and Liao JK (2004) Risk of coronary artery disease associated with polymorphism of the cytochrome P450 epoxygenase CYP2J2. *Circulation* **110**:2132-2136.

Wang H, Jiang Y, Liu Y, Lin C, Cheng G, Chen X, Hao B, Tan W, Lin D and He F (2006) CYP2J2*7 single nucleotide polymorphism in a Chinese population. *Clin. Chim. Acta* **365**:125-128.

Wu S, Moomaw CR, Tomer KB, Falck JR and Zeldin DC (1996) Molecular cloning and expression of CYP2J2, a human cytochrome P450 arachidonic epoxygenase highly expressed in heart. *J. Biol. Chem.* **271**:3460-3468.

Yu Z, Huse LM, Adler P, Graham L, Ma J, Zeldin DC and Kroetz DL (2000) Increased CYP2J2 expression and epoxyeicosatrienoic acid formation in spontanous hypertensive rat kidney. *Mol. Pharmacol.* **57**:1011-1020.

Footnotes:

Financial support:
This work was supported by RO1 ES10855-05 from the National Institute of Environmental Health Sciences and in part by the Intramural Research Program at the NIH, NIEHS (DCZ).

Reprint requests:
Andrea Gaedigk, PhD
Children's Mercy Hospital
Div Clinical Pharmacology
2401 Gillham Road
Kansas City, MO 64108
Email: agaedigk@cmh.edu

Legends for Figures

Figure 1

Expression of CYP2J2 mRNA in human tissues during development.

QRT-PCR was performed on 15 ng total RNA in triplicate reactions. Serial dilutions of a *CYP2J2* amplicon served as a standard to generate a calibration curve ranging from 10^2 to 10^7 copies. Transcript numbers were calculated from log-linear regression analysis of the calibration curve and normalized for 18S ribosomal RNA content.

A: Expression in human fetal and postnatal liver. The genotype of each sample is as indicated in the inset. The 127 fold-variation within the fetal samples decreased to 8-fold upon exclusion of four samples with the lowest transcript numbers (circled). These samples were found to contain low levels of RNA, protein and activity in a previous study (Leeder et al., 2005). EGA, estimated gestational age. There is no significant difference between the pre-and postnatal groups (p=0.82; circled samples excluded, p=0.17). The circled samples are significantly different (p=0.001).

B: Expression in extra-hepatic tissues. Each tissue is coded by a symbol as given in the inset. Liver samples are shown for comparison. Heart and intestine are not significantly different from liver (p=1.0 and 0.14). Lung and kidney are comparable (p=1.0), but differ significantly from liver (p=0.001).

Figure 2

Relationship between CYP2J2 mRNA expression and genotype.

The figure shows the relationship between the number of transcripts/ng total RNA and the presence of zero (0), one (1) or two (2) *CYP2J2*7* alleles. There was no significant difference between samples with zero and one *CYP2J2*7* alleles regardless whether the four samples with low transcript numbers were included (p=0.71) or excluded (p=0.37). No *CYP2J2*2-*6* allelic variants were found. The graph contains fetal and postnatal samples. The samples circled in Figure 1A are shown with open circles; the bar indicates the mean transcript number.

Figure 3

CYP2J2 immunoreactive protein in fetal and postnatal liver. A representative set of samples ranging from 11.1 to 32 weeks EGA and 5 days to 17 years postnatal age are shown. Each lane contained 4 µg microsomal protein, the first and last lanes contained 0.1 pmol recombinant CYP2J2 protein as a positive control. Sample CMM1153, which exhibits a pattern that is more consistent with that observed in the postnatal samples, was loaded on both blots as a reference for band patterns. Membranes containing the fetal and postnatal samples were exposed for 30 and 10 seconds, respectively.

A: detection of immunoreactive protein with anti-CYP2J2rec

B: detection of immunoreactive protein with anti-CYP2J2pep3

JPET Fast Forward. Published on July 25, 2006 as DOI: 10.1124/jpet.106.109215
This article has not been copyedited and formatted. The final version may differ from this version.

Figure 4

Variability of fetal CYP2J2 immunoreactive protein and relationship between protein content and mRNA expression.

Each lane contained 4 µg microsomal protein. Anti-CYP2J2 antibody was used for panels A and B.

Immunoblot with representative samples demonstrating the range of immunoreactive protein observed. For descriptive purposes, 'low', 'intermediate' and 'high' protein categories were assigned by visual inspection. There was no relationship between genotype and amount of protein observed.

Figure 5:

Expression of *CYP2J2* splice variants. Two sets of tissues, one from a postnatal (17 year old) and one from a fetal (22 wks estimated gestational age) male, were utilized for alternate splice variant analysis. Each reaction contained cDNA corresponding to 40 ng total RNA.

A: Full-length cDNA (SV1) was the major amplification product in each tissue analyzed. Minor variants were visible across the panels. M, 1 kb ladder (A); control, amplification from a plasmid mix containing the exon 2 and exon 7 deletions.

B: Graphic display of alternate splice variants identified by cloning and sequencing. Primer locations are as indicated. Boxed depict exons. Transcript-specific PCR for the exon 2 deletion variant (SV4) did not produce any visible product (not shown).

Table 1 Primer sequences and PCR reaction conditions

Primer name	Position AF272142	Primer Sequence	PCR (bp)	Application	Anneal °C	PCR details
10 F	6007-6026	5’ GAA GAG CAG GAG GAC GTC TG	1572	full length cDNA	59	REDAccuTaq LA
11 R	39147-39168	5’ GTC TTC TTA CTT TCC TTG CCC C				
28 F	6223-6240	5’ CAC CTG GAG GTT CAG CTG	194, 357	SV4 detection (see Fig 4)	58	REDTaq
15 R	21012-21033	5’ CTT GAA ATG AGG GTC AAA AGG C				
16 F	24969-24988	5’ GGC CCT CTA CCC AGA AAT CC	188, 376, 527	SV2+3 detection (see Fig 4)	66	REDTaq
19 R	38959-38976	5’ CTG TTC TCC GAG GCA TGC				
14 F	16807-16832	5’ CCC CTA TGC GAG AAC ATA TCT TTA AG	209	QRT-PCR	61	REDTaq
15 R	21012-21033	5’ CTT GAA ATG AGG GTC AAA AGG C				
3 F	20426-20448	5’ GGA ATC AGA ATA CTG TAA TGT TG	669	*2 and *4 genotyping	57	REDTaq
4 R	21075-21094	5’ GGT ACT CAA AGC GTT CTC CG				2 mM $MgCl_2$
3 F	20426-20448	5’ GGA ATC AGA ATA CTG TAA TGT TG	307	*3 genotyping	57	REDTaq
5 R	20703-20732	5’ CTA TCT TCC ATT CCT AGC ACA GTG CT**a tGC**				3 mM $MgCl_2$
6 F	27698-27718	5’ GAA CCC TTC CCT CTT TAC CAG	244	*5 genotyping	60	REDTaq
7 R	27921-27941	5’ CCC TAA AAG ATG GGC TTG AAG				
8 F	31609-31627	5’ CCC CTC TGC ATA GGT GTG C	240	*6 genotyping	60	REDTaq
9 R	31831-31848	5’ CCC TGG ACT CCC ACA CAC				
1 F	5764-5782	5’ GAT TGA ACC GAA CAG AGG C	355	*7 genotyping	60	REDTaq
2 R	6101-6118	5’ GCA GAA AGG CGA CAG TGC				1 mM $MgCl_2$

Table 1 continued

30 F 31 R	1481-1507 6775-6796	5’ TTC ACA CTG AGC ATC TAG CAA TTT GTC 5’ CTG CAT CAA GAA GGG TCC CAG G	5316	seq template upstream, exon 1	62	REDAccuTaq LA
34 F 37 R	16168-16190 21565-21589	5’ AGG CAT GTA CCA CCA TAC CCA GC 5’ AGA GCA ACC AGC ACA GAT GAC TCT C	5422	seq template exons 2, 3, 4	68	Platinum Taq High Fidelity, 5% DMSO
38 F 41 R	22358-22384 28363-28389	5’ GCA TCT ATG CCC TAC TAC CAC ATT CCC 5’ ACA CCA GCA TTA ATA TGA TGT TGT CCC	6032	seq template exons 5, 6, 7	60	REDAccuTaq LA
44 F 45 R	31201-31224 39916-39940	5’ GGG GTG CCA TGT ACT AGA CAT TGG 5’ CAA GAA AAG ATC ACA CCC ACC ATC G	8740	seq template exons 8 and 9	65	REDAccuTaq LA
75-F 55 R	16782-16809 16992-17011	5’ CAA AAC TTT GGG AAC CGC CCC GT**G ggC C** 5’ AGG GAG TGA CTT CAA TCA GG	230	*10 Exon 2 SNP genotyping	58	REDTaq
74 F 46 R	5416-5443 5592-5611	5’AAC AAA TGT TAA TTA AGC ACT TA**T cAT G** 5’ TCT CGG TAG TCT CAT CTT GC	196	Upstream SNP genotyping	52	REDTaq

The table gives the name, sequence and position (GenBank accession AF272142) of each primer. Primers are shown in pairs as they were used for different applications (cDNA amplification, quantitative PCR, genotyping or generation of sequencing template). The lengths of respective PCR amplicons are shown in base pairs (bp) and annealing temperatures for each reaction are given in ºC. Longer amplicons were generated with either the JumpStart REDAccuTaq LA DNA Polymerase Mix (REDAccuTaq LA) or Platinum Taq High Fidelity using their accompanying buffer. Shorter amplicons were amplified with JumpStart REDTaq DNA Polymerase (REDTaq) and the buffer provided. Some reactions were supplemented with $MgCl_2$ or DMSO with final concentrations as indicated. For additional details, please see text.

Table 2 PCR-RFLP-based *CYP2J2* genotyping assays

Allele	Enzyme	PCR in bp	Digest °C	wild-type pattern in bp	variant pattern in bp
*2	*Hpy*188I	669	37	350+108+102+84+18+7	434+108+102+18+7
*3	*Nsi*I	307	37	280 + 27	141 + 139 + 27
*4	*Tsp*509I	669	65	379 + 290	379 + 253 + 37
*5	*Mse*I	244	37	214 + 30	174 + 40+ 30
*6	*Tsp*509I	240	65	157 + 83	240
*7	*Alu*I	355	37	301 + 54	165 + 136 + 54
*10	*Apa*I	230	25	202 + 28	230

Primer sequences and other PCR details are given in Table 1. Each reaction contained 2.5U restriction enzyme and the appropriate accompanying restriction buffer that was diluted 20-fold to a final concentration 0.5x. Digestion reactions were incubated >6 hrs or overnight to ensure completeness.

JPET Fast Forward. Published on July 25, 2006 as DOI: 10.1124/jpet.106.109215
This article has not been copyedited and formatted. The final version may differ from this version.

Table 3 Automated splice site analysis.

Exon	Splice Acceptor Site	Position AF272142	Splice Donor Site	Position AF272142
Exon 1	n/a	n/a	6.9	6241
Exon 2	6.0	16676	9.9	16840
Exon 3	13.6	20464	8.7	20615
Exon 4	14.6	21007	11.3	21169
Exon 5	7.1	22815	10.6	22993
Exon 6	3.7	24849	10.8	24992
Exon 7A	10.0	27718	8.7	27907
Exon 7B	9.0	28260	5.2	28412
Exon 8	9.6	31673	10.6	31813
Exon 9	13.0	38950	n/a	n/a

Splice acceptor and donor site strengths are given in bits. The current model is based on the Human Genome Sequence (Build 33) available at https://splice.cmh.edu. The position of the splice site is indicated in reference to GenBank accession AF272142 and as defined.

JPET Fast Forward. Published on July 25, 2006 as DOI: 10.1124/jpet.106.109215
This article has not been copyedited and formatted. The final version may differ from this version.

Figure 1

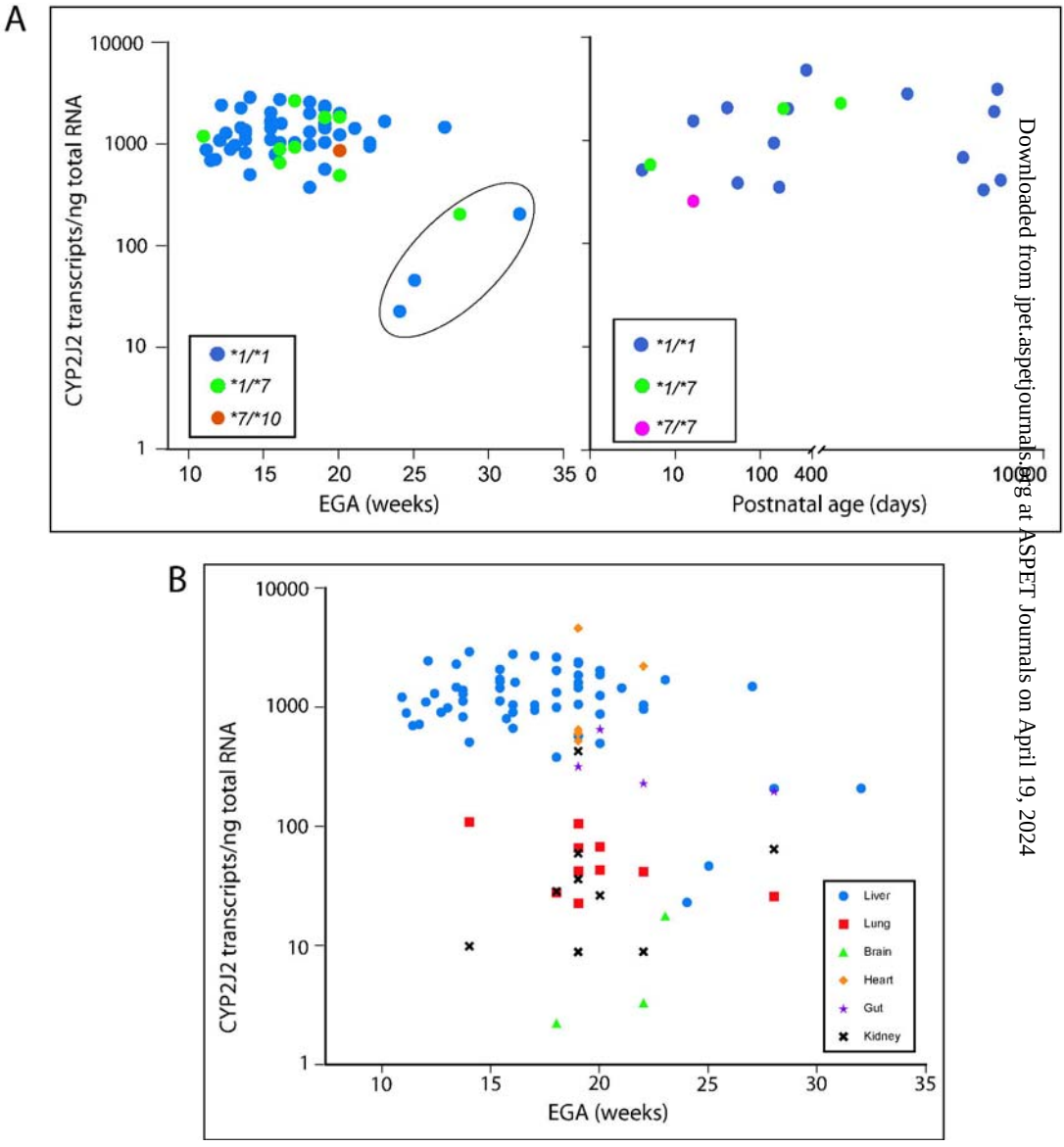

JPET Fast Forward. Published on July 25, 2006 as DOI: 10.1124/jpet.106.109215
This article has not been copyedited and formatted. The final version may differ from this version.

Figure 2

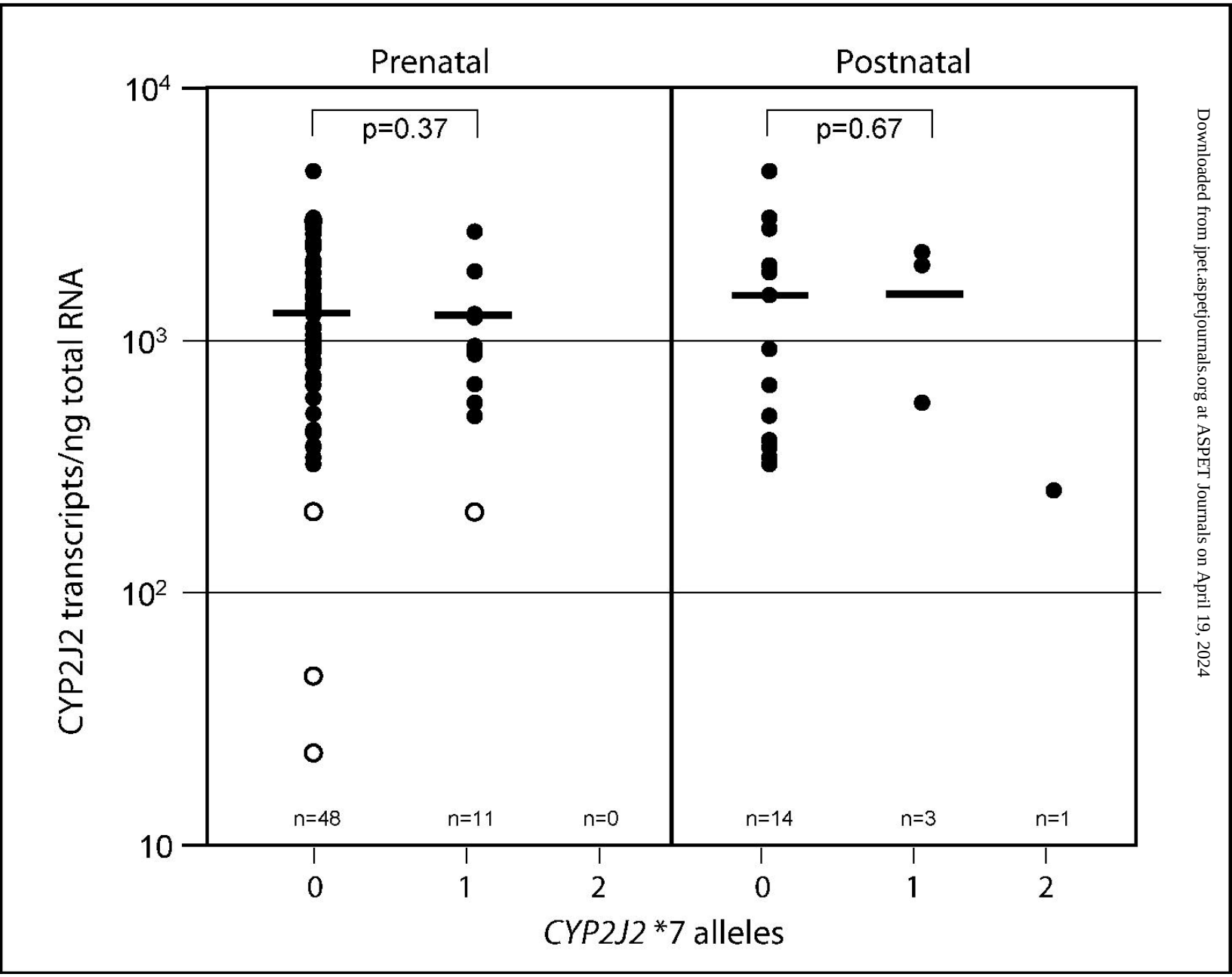

JPET Fast Forward. Published on July 25, 2006 as DOI: 10.1124/jpet.106.109215
This article has not been copyedited and formatted. The final version may differ from this version.

Figure 3

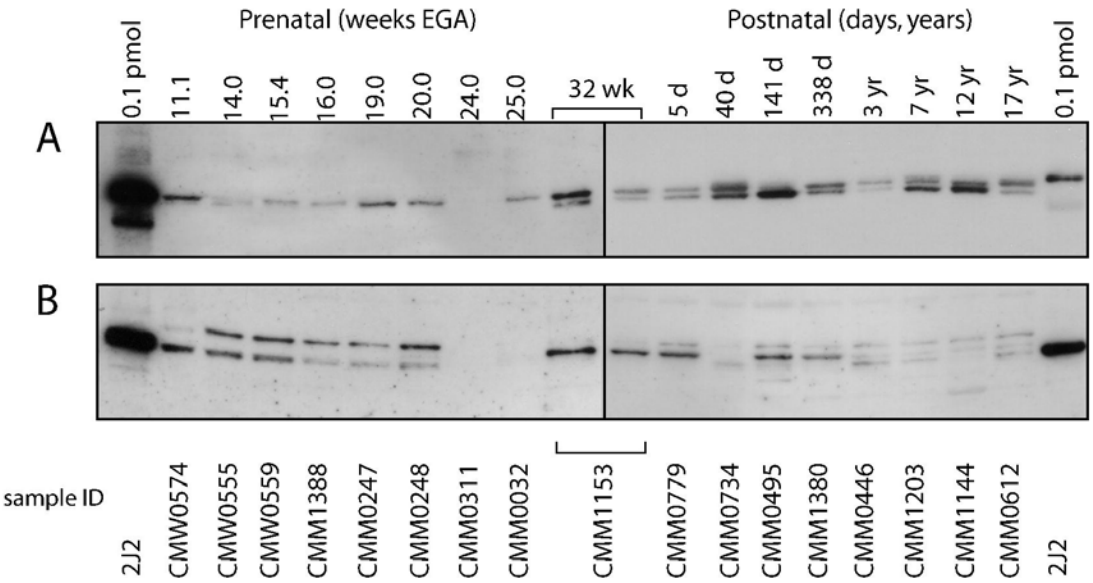

JPET Fast Forward. Published on July 25, 2006 as DOI: 10.1124/jpet.106.109215
This article has not been copyedited and formatted. The final version may differ from this version.

Figure 4

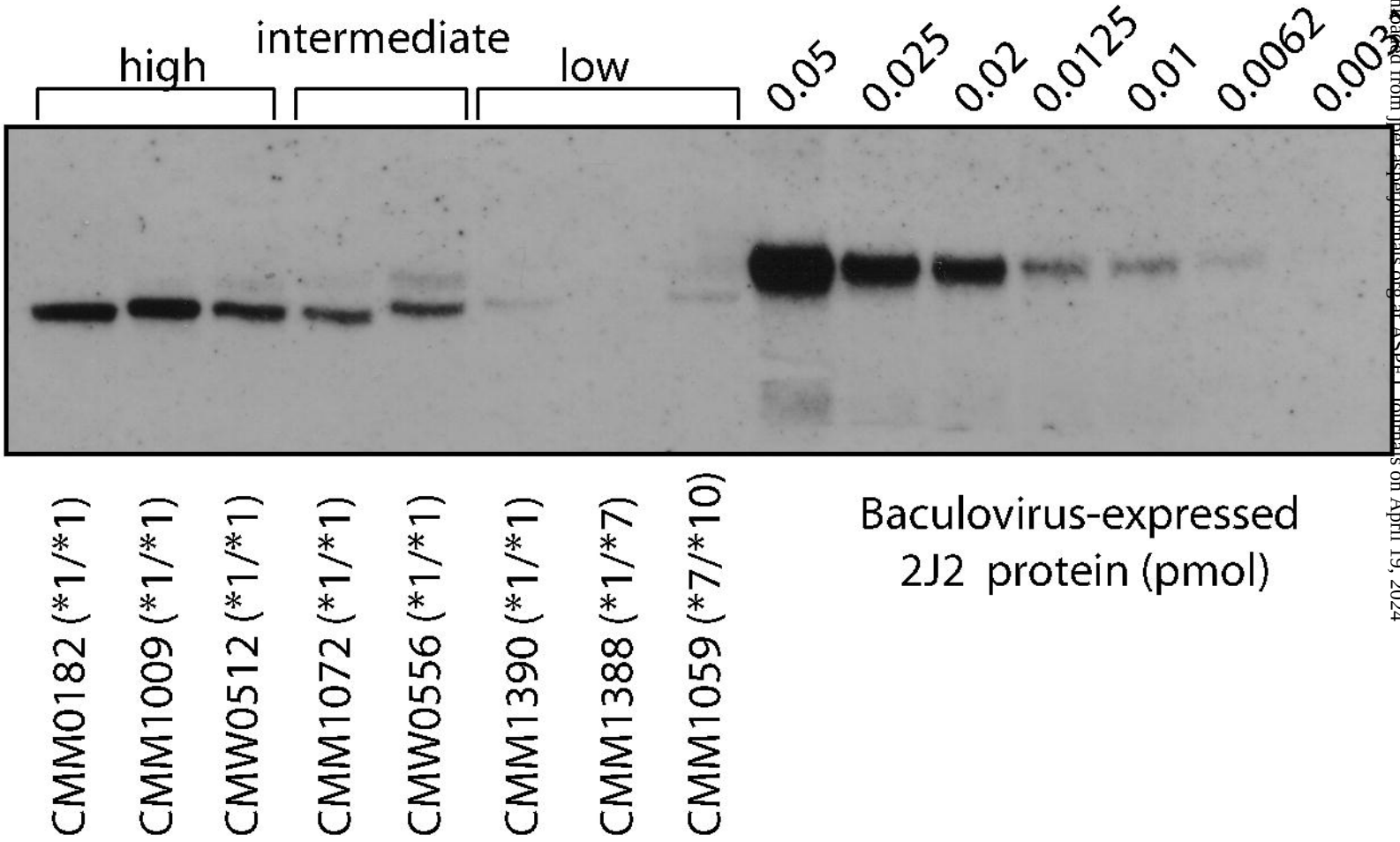

JPET Fast Forward. Published on July 25, 2006 as DOI: 10.1124/jpet.106.109215
This article has not been copyedited and formatted. The final version may differ from this version.

Figure 5